Lab on a Chip

RSC Publishing

COMMUNICATION

View Article Online
View Journal | View Issue

Ultrafast cell switching for recording cell surface transitions: new insights into epidermal growth factor receptor signalling†

Cite this: *Lab Chip*, 2013, **13**, 1031

Received 23rd November 2012,
Accepted 11th January 2013

DOI: 10.1039/c3lc41297k

www.rsc.org/loc

Ya-Yu Chiang[a] and Jonathan West*[ab]

A pinched-flow deflection technology was developed for rapid single cell switching between biochemical microenvironments. Millisecond switching was used to stimulate and preserve epidermal growth factor receptor (EGFR) autophosphorylation transitions. Intramolecular phosphorylation initiates signal transduction, is silenced by phosphatase activity until EGFR dimerization enables intermolecular phosphorylation to initiate downstream signalling.

Introduction

The interface between the cell surface and its microenvironment represents the communication front for signal transduction, information processing and the emergent behaviour of the biological system. Surface processes are fast, occurring over sub-second timescales. To resolve the detail within these processes, methods enabling near-instantaneous system perturbation are required and should ideally be combined with real-time reaction monitoring. The electronic quality of voltage-gated ion channel processes is highly convenient for rapid signal delivery and rapid response recording.[1] No such convenience exists for biochemically-mediated cell surface communication processes; the timescales for mixing μL to mL volumes (ESI† Video 1) and camera exposure periods necessary to observe fluorescent reporters are of the order of a second, far exceeding the timescales of the mechanisms under investigation.

Although miniaturisation can be used to shrink mass transfer distances, mixing remains problematic in microscopic flows with characteristically low Reynolds and low Péclet numbers. Here cells and biomolecules are confined to their respective laminar streams with interactions confined to the virtual interface by diffusion-limited mass transfer.[2] Alternatively, turbulent flows can be generated by high velocity transport through narrow orifices to rapidly stretch and fold material lines to attain milli- to microsecond mixing timescales.[3] In the quenched-flow format, this is used for rapid reaction triggering and, following a defined incubation, rapid reaction arrest to preserve intermediates for downstream analysis.[4] Although well equipped for investigating solution phase molecular kinetics, the high-shear conditions disrupt cell membranes and prevent meaningful investigation of membrane-hosted events. As a consequence of the different drawbacks, the molecular dynamics and mechanisms underpinning critical cell–ligand interactions cannot be resolved and remain poorly understood.

In place of conventional (micro)mixing, the cells can instead be transported across the virtual interface between laminar flows. Numerous actuation techniques are available; for example, optical,[5] acoustic[6] and dielectric[7] force fields can be positioned orthogonal to the flow for cell deflection. However, the various approaches do not scale favourably and with weak cell–medium material contrasts exert only pN forces. As a result, whole cell switching requires many 10's of milliseconds, inadequate to resolve membrane-hosted molecular processes. In contrast passive systems, either hydrodynamic filtration[8] or deterministic lateral displacement (DLD) configurations, involving angled pillar arrays[9] or pinched-flow[10] elements, can be used to shrink laminar stream widths beneath the cell radius to rapidly deflect cells into neighbouring laminar streams. These systems have been almost exclusively used for size- and shape-based[11] bioparticle fractionation, with the exception of platelet labelling, *E. coli* lysis[12] and isolating nuclei.[13] In this contribution we present an innovative quenched-flow architecture comprising two pinched-flow deflection elements separated by a channel length corresponding to the incubation dwell time. The cell switching system was used to stimulate and record the molecular transitions underpinning epidermal growth factor receptor (EGFR) signal transduction.

Principles and methodology

The microfluidic design and continuous-flow single cell deflection concept are illustrated in Fig. 1. Devices were replicated in PDMS

[a]*Leibniz-Institut für Analytische Wissenschaften – ISAS – e.V., 44227 Dortmund, Germany. E-mail: yychiang@mems.iam.ntu.edu.tw*
[b]*Institute for Life Sciences, University of Southampton, SO17 1BJ, UK. E-mail: J.J.West@soton.ac.uk; Tel: +44 2380 593460*

† Electronic supplementary information (ESI) available: Magnetic mixing and cell deflection videos, Materials and Methods, CAD files, replicate pY1173 dynamics data. See DOI: 10.1039/c3lc41297k

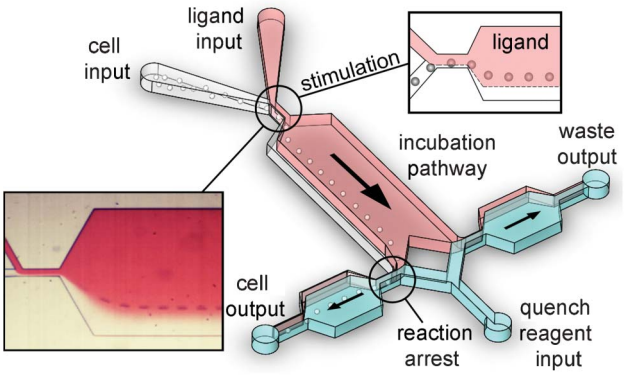

Fig. 1 Pinched-flow deflection principle (inset, right, adapted from Yamada *et al.*[10a]) and single cell deflection into a stream doped with red dye (inset, left). Microfluidic architecture for 2-step cell submersion into a ligand stream (pink) and then into a quench buffer stream (blue).

to a depth of 60 μm and packaged as previously reported.[14] The pinched-flow stream thinning elements were 200 μm-long, 25 μm-wide and interfaced to 500 μm-wide expansion channels for 20-fold amplification of the initial displacement (see ESI† CAD files). Full details of device fabrication and operation, cell culture and EGFR analysis can be found in the ESI† Materials and Methods. To achieve deflection into the stimulant stream, the cell radius r must exceed the width of the cell stream w_{CS} (*i.e.* $r > w_{CS}$). HeLa S3 epithelial cells‡ were used in this study and have a mean radius of 7.9 μm (SD ± 1.1). A ligand to cell stream flow ratio of 7 : 1 was used. Together with the parabolic flow field this produced a cell stream 4.0 μm in width. The spherical cell morphology is not deformed, resulting in the mean cell centre being deflected 3.9 μm (*i.e.* $r > w_{CS}$) across the virtual interface into the ligand stream. This is further amplified (20-fold) in the expansion channel to ensure each cell is fully submerged in the ligand stream. The total deflection distance D of each cell across the virtual interface can be expressed as:

$$D = (r - w_{CS}) \times {}^{w_{exp}}/_{w_{STE}} \quad (1)$$

where w denotes the width of the expansion channel (exp) or the stream thinning element (STE).

Ultrafast cell switching

Continuous flow single cell deflection was highly reliable (see, ESI† Video 2). A mean flow velocity of 100 mm s^{-1} was used for cell stimulation by EGF (at saturating levels; 100 ng mL^{-1}).[2] Channel bifurcation and the use of a 7 : 1 quench buffer to cell flow ratio, produced a 400 mm s^{-1} mean velocity at the second STE (Re_{max}= 0.016). A high speed camera (EoSens® mini2, Mikrotron GmbH, Germany) operating with a 10 000 fps capture rate was used to measure the stimulation switch time $\tau_{stim.}$ required for complete cell submersion in the ligand stream. Images of a HeLa cell entering, travelling through and exiting from the 200 μm-long STE are documented in Fig. 2(A). Plotted in Fig. 2(B), the mean $\tau_{stim.}$ was 2.22 ms (SD ± 0.15, or FWHM ± 0.27). Cell transport in the

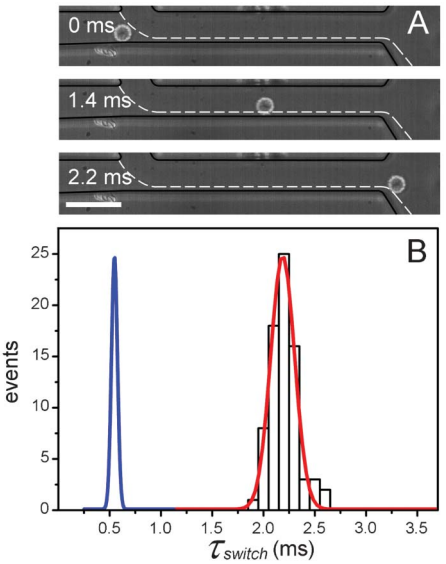

Fig. 2 High speed imaging frames documenting the transport of a single HeLa S3 cell through a STE at ~100 mm s^{-1} (A). Scale bar is 30 μm. Measured $\tau_{stim.}$ (red) with Gaussian curve fitting (r^2 = 0.99) and extrapolated τ_{quench} (blue) values (B).

quench STE was too fast for object-triggered imaging. The τ_{quench} was instead extrapolated from the τ_{stim} data and estimated to be 0.55 ms (a 4-fold velocity increase forms the basis of our extrapolation). Faster switch times can be achieved by truncating the STE length. Nevertheless, the present milli- and sub-millisecond pinched-flow deflection switch times are ~1000-fold faster than stimulation times obtained by traditional mixing methods,[15] 10–100 faster than the use of actuation force fields,[5–7] faster than hydrodynamic filtration[8] and equivalent to those involved in the analysis of molecular kinetics by stopped- and quenched-flow techniques. Importantly, operation in the laminar regime, without turbulence, preserves the integrity of the cell membrane and opens the possibility to investigate ligand-mediated cell surface processes with unprecedented temporal resolution.

EGFR autophosphorylation dynamics

The epidermal growth factor receptor (EGFR) is a transmembrane receptor tyrosine kinase (RTK) involved in normal development and pathologic scenarios, notably cancer.[16] EGFR contains an extracellular domain for binding ligands, such as EGF and transforming growth factor alpha (TGF-α), and an intracellular kinase domain. The contemporary activation model involves receptor–ligand association which causes the transition from an inactive monomeric form to an activated state, able to dimerize for asymmetric intermolecular (*trans*) auto-phosphorylation.[17] Association with the phosphotyrosine-binding SH2 domains of other proteins elicits signal transduction cascades, such as MAPK, Akt and JNK pathways that lead to DNA synthesis and cell proliferation.[18]

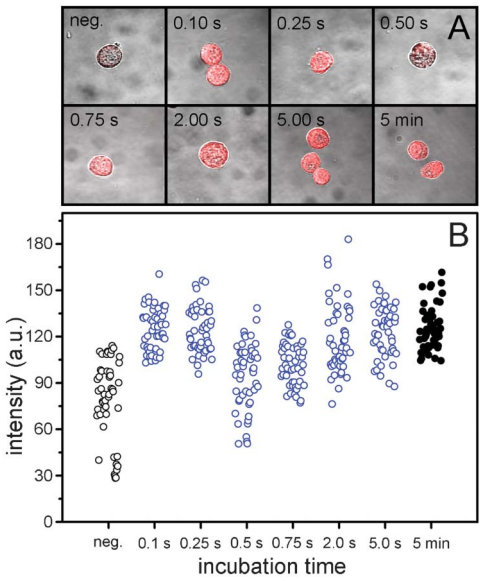

Fig. 3 EGFR Y1173 autophosphorylation dynamics. Choice images of single cells immunostained for pY1173 for the different zero to 2.0 s on-chip EGF stimulations. Incubations for 5 s and 5 min were achieved by straightforward mixing in 2 mL volumes. Negative control cells were combined, on chip, with serum-free media only (A). Single cell pY1173 heterogeneity throughout the time course (B). Mean data is plotted with a linear time scale in Fig. 4. Results from replicate experiments are provided in the ESI† Fig. 1.

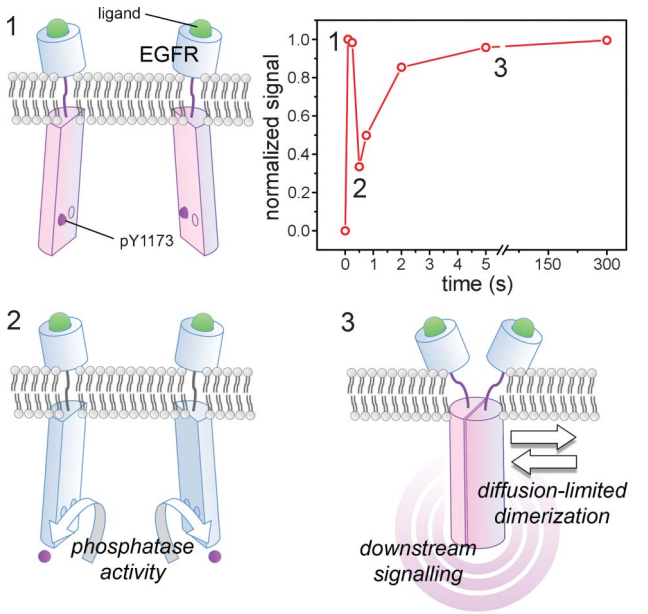

Fig. 4 EGFR Y1173 population-averaged autophosphorylation dynamics (top, right). Proposed signalling mechanism: EGF-directed *cis* phosphorylation (1); negative feedback regulation involving phosphatase activity (2); diffusion-limited dimerization producing a phosphatase resistant complex able to *trans* phosphorylate and evoke downstream signalling (3).

Ligand-mediated receptor transitions occurring within sub-second timescales were previously inaccessible. In this study we have used the microfluidic switch technology for the quenched-flow analysis of EGF-mediated tyrosine 1173 auto-phosphorylation. Single cells were immunostained for pY1173, with area mean grey value measurements used to quantify phosphorylation levels. Single cell EGFR Y1173 phosphorylation data from incubation-grouped sub-populations are documented in Fig. 3. There was marked heterogeneity of the pY1173 signal from the different sub-populations ($n > 50$ per incubation period). Single cell heterogeneity is rooted in the noise caused by stochastic fluctuations in the signalling networks and possibly by the constitutively activated EGFR homolog, ErbB2.[19] Despite the fluctuations within the cell population a clear ($p < 10^{-12}$) pY1173 biphasic signal was observed and is shown in Fig. 4: Complete Y1173 phosphorylation occurs within 100 ms, and is maintained for $\geqslant$250 ms, followed by dephosphorylation towards baseline levels at 500 ms and asymptotic recovery to saturation levels over a $\sim$5 s timescale.

The initial pY1173 signal followed by the sharp dephosphorylation transition was previously hidden by the low time resolution of existing methods. The data provides new insights, adding complexity to the widely accepted autocatalytic mechanism which considers dimerization a pre-requisite for allosteric EGFR auto-phosphorylation.[17,20] Instead the results point to a new origin of signalling involving intramolecular phosphorylation with activation shortly suppressed by dephosphorylation, most likely by SHP-1, a Y1173-specific protein tyrosine phosphatase (PTP).[21] The asymptotic recovery of the pY1173 signal in a $\sim$5 s timeframe is a hallmark feature of dimerization-mediated EGFR activation with kinetics defined by diffusion-driven collision probability within the membrane.[22] The pY1173 protection mechanism is unknown, but may involve displacement of the phosphatase during EGFR dimerization and steric shielding of the Y1173 residue to prevent repeated dephosphorylation. Taken together the results may imply a novel negative feedback regulatory mechanism, silencing *cis* phosphorylation until diffusion-mediated collision with another ligand-occupied monomer for the initiation of *trans* phosphorylation necessary to initiate downstream signalling. This putative mechanism is illustrated in Fig. 4 along with the population-averaged autophosphorylation dynamics.

The proposed mechanism can be used to lend weight to the selection of anti-cancer targets and desired modes of therapeutic action. Importantly, the microfluidic switch technology allows whole cell investigations, providing truly authentic receptor and cell surface models[23] with freedom to interact with molecular players present in either membrane or cytosolic compartments.

Conclusions

In this paper we have demonstrated an ultrafast cell switching platform which can be used to peer within the 10–1000 ms window to gain new insights into the mechanisms underlying ligand-cell interactions. This is the first report of biphasic EGFR signalling, and implicates *cis* phosphorylation counter-balanced by dephosphorylation, prior to dimerization and protected *trans* phosphorylation for downstream signalling. The temporal resolving power of the microfluidic cell switching technology can be further harnessed for the deeper investigation of a tremendous spectrum of other cell surface processes.

Acknowledgements

We gratefully acknowledge Ulrich Marggraf (ISAS) for SU-8 fabrication, Norman Ahlmann (ISAS) for constructing temperature control elements and Sarah Waide (ISAS) for support with cell handling. Fluorescent imaging was undertaken with the support of Sven Müller and Jian Hou at the MPI for Molecular Physiology, Dortmund. René Zahedi (ISAS), Eli Zamir (MPI), Boris Kholodenko (University College Dublin), Phil Williamson, Jörn Werner and Ivo Tews (UoS) are credited for valuable biochemistry discussions. The research was financially supported by the DFG (WE3737/3-10) and by the Ministerium für Innovation, Wissenschaft und Forschung des Landes Nordrhein-Westfalen. YYC thanks the Taiwanese Ministry of Education for her Ph.D. scholarship.

References

‡ HeLa S3 cells cultured in suspension retain signalling functionality.[2]

1 E. Neher and B. Sakmann, *Nature*, 1976, **260**, 799–802.
2 J. Dengjel, V. Akimov, J. V. Olsen, J. Bunkenborg, M. Mann, B. Blagoev and J. S Andersen, *Nat. Biotechnol.*, 2007, **25**(5), 566–568.
3 S. E. Kurzawa and M. A. Geeves, *J. Muscle Res. Cell Motil.*, 1996, **6**, 669–676.
4 A. R. Fersht and R. Jakes, *Biochemistry*, 1975, **14**(15), 3350–3356.
5 (*a*) P. Y. Chiou, A. T. Ohta and M. C. Wu, *Nature*, 2005, **436**, 370–372; (*b*) E. Eriksson, J. Enger, B. Nordlander, N. Erjavec, K. Ramser, M. Goksör, S. Hohmann, T. Nyström and D. Hanstorp, *Lab Chip*, 2007, **7**, 71–76.
6 M. Evander, A. Lenshof, T. Laurell and J. Nilsson, *Anal. Chem.*, 2008, **80**, 5178–5185.
7 (*a*) S. Fiedler, S. G. Shirley, T. Schnelle and G. Fuhr, *Anal. Chem.*, 1998, **70**, 1909–1915; (*b*) U. Seger, S. Gawad, R. Johann, A. Bertsch and P. Renaud, *Lab Chip*, 2004, **4**, 148–151.
8 M. Yamada, J. Kobayashi, M. Yamato, M. Seki and T. Okano, *Lab Chip*, 2008, **8**, 772–778.
9 L. R. Huang, E. C. Cox, R. H. Austin and J. C. Sturm, *Science*, 2004, **304**, 987–990.
10 (*a*) M. Yamada, M. Nakashima and M. Seki, *Anal. Chem.*, 2004, **76**, 5465–5471; (*b*) J. Takagi, M. Yamada, M. Yasuda and M. Seki, *Lab Chip*, 2005, **5**, 778–784.
11 S. H. Holm, J. P. Beech, M. P. Barrett and J. O. Tegenfeldt, *Lab Chip*, 2011, **11**, 1326–1332.
12 K. J. Morton, K. Loutherback, D. W. Inglis, O. K. Tsui, J. C. Sturm, S. Y. Chou and R. H. Austin, *Lab Chip*, 2008, **8**, 1448–1453.
13 K. Toyama, M. Yamada and M. Seki, *Biomed. Microdevices*, 2012, **14**, 751–757.
14 J.-P. Frimat, M. Becker, Y.-Y. Chiang, D. Janasek, J. G. Hengstler and J. West, *Lab Chip*, 2011, **11**, 231–237.
15 G. Moehren, N. Markevich, O. Demin, A. Kiyatkin, I. Goryanin, J. B. Hoek and B. N. Kholodenko, *Biochemistry*, 2002, **41**, 306–320.
16 K. Oda, Y. Matsuoka, A. Funahashi and H. Kitano, *Mol. Syst. Biol.*, 2005, **1**(1), 2005.0010, DOI: 10.1038/msb4100014.
17 (*a*) J. H. Bae and J. Schlessinger, *Mol. Cells*, 2010, **29**, 443–448; (*b*) N. F. Endres, K. Engel, R. Das, E. Kovacs and J. Kuriyan, *Curr. Opin. Struct. Biol.*, 2011, **21**, 777–784.
18 G. Carpenter and S. Cohen, *J. Biol. Chem.*, 1990, **265**, 7709–7712.
19 J. E. Ladbury and S. T. Arold, *Trends Biochem. Sci.*, 2012, **37**(5), 173–178.
20 (*a*) R. Hazan, B. Margolis, M. Dombalagian, A. Ullrich, A. Zilberstein and J. Schlessinger, *Cell Growth Diff.*, 1990, **1**, 3–7; (*b*) B. Margolis, N. Li, A. Koch, M. Mohammadi, D. R. Hurwitz, A. Zilberstein, A. Ullrich, T. Pawson and J. Schlessinger, *J. Biol. Chem.*, 1989, **264**, 10677–10680.
21 (*a*) H. Keilhack, T. Tenev, E. Nyakatura, J. Godovac-Zimmermann, L. Nielsen, K. Seedorf and F. D. Bohmer, *J. Biol. Chem.*, 1998, **273**, 24839–24846; (*b*) T. Tiganis, *Life*, 2002, **53**, 3–14.
22 P. J. Verveer, F. S. Wouters, A. R. Reynolds and P. I. H. Bastiaens, *Science*, 2000, **290**, 1567–1570.
23 N. J. Bessman and M. A. Lemmon, *Nat. Struct. Mol. Biol.*, 2012, **19**(1), 1–3.

